Engineering Fracture Mechanics 132 (2014) 169–176

Contents lists available at ScienceDirect

Engineering Fracture Mechanics

journal homepage: www.elsevier.com/locate/engfracmech

T-stress effects on crack kinking in Finite Fracture Mechanics

Pietro Cornetti, Alberto Sapora *, Alberto Carpinteri

Department of Structural, Geotechnical and Building Engineering, Corso Duca degli Abruzzi 24, 10129 Torino, Italy

ARTICLE INFO

Article history:
Received 14 July 2014
Received in revised form 20 September 2014
Accepted 7 October 2014
Available online 19 October 2014

Keywords:
Brittle materials
Crack kinking
T-stress
Finite Fracture Mechanics

ABSTRACT

Finite Fracture Mechanics (FFM) is a coupled criterion based on the contemporaneous fulfilment of the energy balance and a proper stress requirement. When dealing with mixed-mode brittle fracture of cracked elements, *T*-stress affects both the conditions. In the present work, the problem is investigated as the mode mixity varies. Results are provided in terms of the critical stress intensity factors and the critical kinking angle, by referring to two different definitions of dimensionless *T*-stress, depending on which mode (*I* or *II*) dominates. This novel approach is validated by a comparison with PMMA experimental data available in the Literature.

1. Introduction

The discrepancy, observed between classical fracture criteria predictions [1,2] and different experimental data, has motivated the research on *T*-stress effects in mixed-mode brittle fracture of cracked structures for approximately the last forty years [3–14].

Indeed, former studies were generally devoted to analyze the *T* influence on the stress field and strain energy release rate in the neighborhood of the crack tip. It was only in the middle of nineties, that failure criteria based on a linear-elastic analysis combined with an internal material length were successfully proposed in this framework. Among these, the point stress criterion represents undoubtedly the simplest and most implemented approach. In the spirit of the works by Williams and Ewing [3] and Ritchie et al. [15], it was put forward in [16,17] and later developed and applied to different experimental data in [18,19]. Nonlocal (average) stress and energy criteria were formalized by Seweryn [17] (see also [20] for considerations on the latter).

More recently, also the coupled approach proposed by Leguillon [21] was modified to include *T*-stress effects [22]. The analysis was carried out numerically, by a two-scale asymptotic matching procedure [23], and it was mainly concerned with the behavior under pure mode *I* conditions: as regards the crack propagation angle, differently from the results presented in [18], a jump was observed for a threshold positive value of *T*.

In the present work, these problems are faced by means of FFM [24,25]: the criterion is similar to that presented in [22], but the stress condition is averaged and not of punctual type. As regards V-notches, the two approaches were found to provide different results, both as concerns the failure load [26] and the crack propagation angle in mixed mode [27]. It is important to remark that according to both the coupled criteria, the crack advance ceases to be a material property and becomes a structural parameter, allowing to remove some inconsistencies related to the criteria previously introduced.

The FFM analysis is carried out by exploiting expressions for the asymptotic stress field and the crack driving force available in the Literature, where the angular functions related to the latter can be found tabulated [28,29]. The coupled equations

* Corresponding author.
E-mail addresses: pietro.cornetti@polito.it (P. Cornetti), alberto.sapora@polito.it (A. Sapora), alberto.carpinteri@polito.it (A. Carpinteri).

http://dx.doi.org/10.1016/j.engfracmech.2014.10.011
0013-7944/

Nomenclature

c	length of a kinked crack
G	crack driving force
G_c	fracture energy
K_I	mode *I* SIF
K_{II}	mode *II* SIF
K_{Ic}	fracture toughness
K_{If}	critical value of mode *I* SIF
K_{IIf}	critical value of mode *II* SIF
K^*_{If}	dimensionless critical value of mode *I* SIF
K^*_{IIf}	dimensionless critical value of mode *II* SIF
K^k_I	SIF related to the kinked crack for mode *I*
K^k_{II}	SIF related to the kinked crack for mode *II*
l_{ch}	characteristic length
T	*T*-stress
β	angular functions related to the SIFs of kinked cracks
ψ	mode mixity
θ	kinking angle
λ_I	mode *I* Williams' eigenvalues
λ_{II}	mode *II* Williams' eigenvalues
σ_u	tensile strength
Δ	finite crack advance
δ	dimensionless crack advance
τ_I	dimensionless *T*-stress with respect to mode *I*
τ_{II}	dimensionless *T*-stress with respect to mode *II*

providing the critical load and kinking angle are derived analytically and then solved numerically. Eventually, observe that differently from the studies carried out in [7,17,18,22], results are presented according to two different definitions of the dimensionless *T*-stress, one more suitable to mode *I*-dominated zone, and one with mode *II*-dominated zone. This synthetic and novel approach allows one to investigate the failure conditions in the extreme cases ($K_I = 0$ and $K_{II} = 0$) at the same time, without loosing of generality.

2. FFM and *T*-stress

Let us consider a cracked element with a polar reference system placed at the notch root (Fig. 1). Finite Fracture Mechanics is based on the assumption of a finite crack extension Δ and on the contemporaneous fulfilment of two conditions. The former is a stress requirement: the average circumferential stress $\sigma_{\theta\theta}(r,\theta)$ on Δ, prior to the crack extension, must be greater than the material tensile strength σ_u. In formulae:

$$\int_0^{\Delta} \sigma_{\theta\theta}(r,\theta)\mathrm{d}r \geqslant \sigma_u \Delta. \tag{1}$$

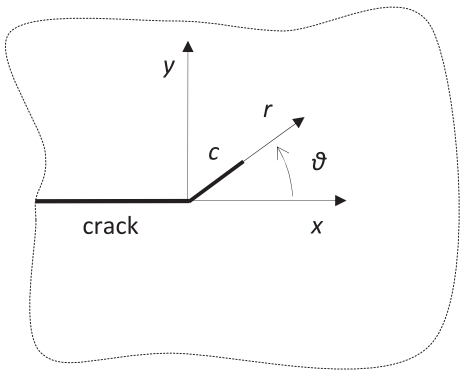

Fig. 1. Cracked element with polar coordinate system and kinked crack of length *c*.

The latter is the energy balance: the integral of the crack-driving force G on Δ, representing the energy available for the crack increment, must be higher than the fracture energy G_c times the crack increment Δ

$$\int_0^{\Delta} G(c,\theta)\mathrm{d}c \geqslant G_c\Delta. \tag{2}$$

By means of the well-known Irwin's relationships, Eq. (2) can be expressed in terms of the stress intensity factors (SIFs) related to the kinked crack, K_I^k and K_{II}^k for mode I and mode II, respectively, and of the fracture toughness K_{Ic}, namely:

$$\int_0^{\Delta} [(K_I^k(c,\theta))^2 + (K_{II}^k(c,\theta))^2]\mathrm{d}c \geqslant K_{Ic}^2\Delta. \tag{3}$$

The FFM criterion is thus described by the coupled inequalities (1) and (3), and in order to be implemented it requires the functions $\sigma_{\theta\theta}$, K_I^k and K_{II}^k. Henceforth the subscripts I and II will always refer to mode I and mode II, respectively, without the necessity of further clarifications.

2.1. Stress field and stress condition

By taking the T-stress effects into account, the circumferential stress field $\sigma_{\theta\theta}(r,\theta)$ at the crack tip can be approximated as (see Fig. 1 with $c = 0$):

$$\sigma_{\theta\theta}(r,\theta) = \frac{K_I}{\sqrt{2\pi r}} f^I_{\theta\theta}(\theta) + \frac{K_{II}}{\sqrt{2\pi r}} f^{II}_{\theta\theta}(\theta) + T\sin^2\theta, \tag{4}$$

where K_I and K_{II} are the SIFs related to the main crack, $f^I_{\theta\theta}$ and $f^{II}_{\theta\theta}$ are two angular functions (see, for instance, [30]), while the third term represents the nonsingular T-stress contribution.

Let us now introduce:

- The functions $\bar{f}^i_{\theta\theta}$ $(i = I, II)$, obtained by multiplying the corresponding functions $f^i_{\theta\theta}$ by a factor $\sqrt{2/\pi}$.
- The mode-mixity $\psi = \arctan(K_{II}/K_I)$. It is independent of the applied load magnitude and it is equal to 0° and to 90°, for mode I and mode II loading conditions, respectively. Indeed, notice that $K_I = 0$ does not represent, strictly speaking, a pure mode II condition since $T \neq 0$ corresponds to a symmetrical load.
- The characteristic length $l_{ch} = (K_{Ic}/\sigma_u)^2$.
- The dimensionless crack advance, $\delta = \Delta/l_{ch}$.
- The dimensionless T-stress (or biaxiality ratio [7]), $\tau_I = T\sqrt{l_{ch}}/K_I$.

Notice that τ_I has been defined with respect to the mode I SIF [7,17,22], although other choices are possible [18]: this point will be discussed more in details in Section 3.

For monotonically increasing $G(c)$ and monotonically decreasing $\sigma_{\theta\theta}(r)$ functions (as in the present case), the lowest load satisfying the inequalities (1) and (2) is achieved when the equal sign holds. Hence, by inserting (4) into (1) and integrating, analytical manipulations yield:

$$\frac{K_I}{K_{Ic}} = \frac{\sqrt{\delta}}{\bar{f}^I_{\theta\theta} + \tan\psi\bar{f}^{II}_{\theta\theta} + \tau_I\sin^2\theta\sqrt{\delta}}. \tag{5}$$

Let us remark that Eq. (5) represents the critical condition for the average stress criterion [17] by assuming $\delta = 2/\pi$: in this case, the crack advance results a material property.

2.2. SIFs for kinked cracks and energy condition

By applying dimensional analysis concepts and the principle of effects superposition, the SIFs related to a kinked crack of length c read [9,10]:

$$K_I^k(c,\theta) = \beta_{11}(\theta)K_I + \beta_{12}(\theta)K_{II} + \beta_1(\theta)T\sqrt{c}, \tag{6}$$

$$K_{II}^k(c,\theta) = \beta_{21}(\theta)K_I + \beta_{22}(\theta)K_{II} + \beta_2(\theta)T\sqrt{c}, \tag{7}$$

supposing that the kinked crack is small enough to lie in the K_I–K_{II}–T dominated region around the main crack. Angular functions β can be found tabulated in the Literature over the range $0° \leqslant \theta \leqslant 90°$, with sufficient accuracy (errors below 1%). Values are provided every 1° as regards β_{ij} [29] and every 10° as regards β [28] (see also [31]). It is important to outline that β_2, β_{12} and β_{21} are odd functions of θ, differently from β_1, β_{11} and β_{22} which result to be even. Moreover, the last term in Eqs. (6) and (7), representing the T-stress contribution, vanishes coherently for a vanishing crack length c.

By substituting Eqs. (6) and (7) into Eq. (3), the energy balance provides:

$$\left(\frac{K_I}{K_{Ic}}\right)^2 = \frac{1}{(\bar{\beta}_{11} + \bar{\beta}_{12}\tan\psi + \bar{\beta}_{22}\tan^2\psi) + \frac{4\tau_I\sqrt{\delta}}{3}(\bar{\beta}_1 + \bar{\beta}_2\tan\psi) + \frac{\tau_I^2\delta}{2}(\beta_1^2 + \beta_2^2)}, \tag{8}$$

where

$$\bar{\beta}_1 = \beta_1\beta_{11} + \beta_2\beta_{21}, \tag{9}$$

$$\bar{\beta}_2 = \beta_1\beta_{12} + \beta_2\beta_{22}, \tag{10}$$

$$\bar{\beta}_{11} = \beta_{11}^2 + \beta_{21}^2, \tag{11}$$

$$\bar{\beta}_{12} = 2(\beta_{11}\beta_{12} + \beta_{21}\beta_{22}), \tag{12}$$

$$\bar{\beta}_{22} = \beta_{12}^2 + \beta_{22}^2. \tag{13}$$

Angular functions $\bar{\beta}$, obtained by interpolating β-values, are reported in Fig. 2: notice that $\bar{\beta}_2$ and $\bar{\beta}_{12}$ are odd functions of θ, the remaining ones being even.

Before proceeding, let us remark that Eq. (8) reverts to the critical condition provided by Linear Elastic Fracture Mechanics (LEFM), leading to the well-known G_{max} criterion, for $\tau_I = 0$. On the other hand, Eq. (8) represents the critical condition for the nonlocal energy approach, put forward in [17] by assuming that the crack extension is a material constant (see also [20]).

2.3. FFM implementation

At incipient failure ($K_I = K_{If}$), Eqs. (5) and (8) become a system of two equations in two unknowns: the critical crack advancement δ_c and the failure load, implicitly embedded in the function K_{If}. The hypothesis that failure takes place when K_I reaches its critical value K_{If} is reasonable within sufficiently brittle structural behavior.

A straightforward substitution of Eq. (5) into (8) provides

$$\delta - \frac{\left(\bar{f}^I_{\theta\theta} + \tan\psi\bar{f}^{II}_{\theta\theta} + \tau_I \sin^2\theta\sqrt{\delta}\right)^2}{(\bar{\beta}_{11} + \bar{\beta}_{12}\tan\psi + \bar{\beta}_{22}\tan^2\psi) + \frac{4\tau_I\sqrt{\delta}}{3}(\bar{\beta}_1 + \bar{\beta}_2\tan\psi) + \frac{\tau_I^2\delta}{2}(\beta_1^2 + \beta_2^2)} = 0 \tag{14}$$

which is an equation in the unique unknown δ, since, once the loading and the structural properties are known, ψ and τ_I are fixed. In order to implement FFM, Eq. (14) has firstly to be solved over the range $0^\circ \le \theta \le 90^\circ$: a different crack advance δ corresponds to a different θ. Each couple (δ, θ) must be then substituted into either Eqs. (5) or (8). By referring to Eq. (5), the actual crack advance δ_c and critical kinking angle θ_c are those which minimize the function

$$K^*_{If} = \frac{\sqrt{\delta_c}}{\bar{f}^I_{\theta\theta} + \tan\psi\bar{f}^{II}_{\theta\theta} + \tau_I \sin^2\theta_c\sqrt{\delta_c}}, \tag{15}$$

where $K^*_{If} = K_{If}/K_{Ic}$ is the dimensionless critical value of mode I SIF.

The problem could be also faced through the mathematical technique of Lagrange multipliers, since we are looking for the couple (δ, θ) which minimizes the function K_{If} (Eq. (5)) under the constraint provided by relationship (14). This technique was exploited to deal with V-notched structures subjected to mixed-mode loading conditions [30].

Once K_{If} is evaluated through Eq. (15), it is possible to obtain K_{IIf} by means of the relationship $K_{IIf} = \tan\psi K_{If}$. Indeed, for a vanishing mode I SIF ($K_I \to 0, \psi \to 90^\circ$), τ_I tends to infinite and the problem results ill-posed. Of course, the roles of K_I and K_{II}

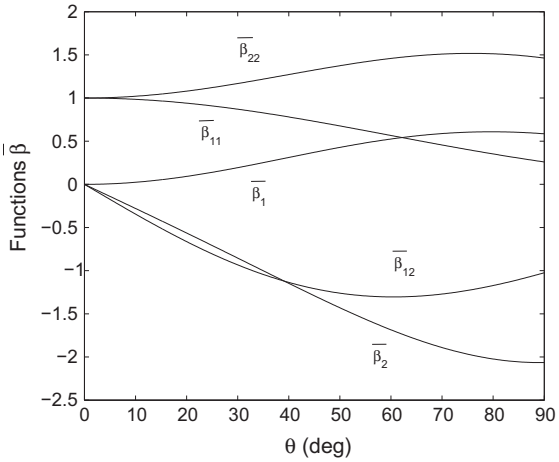

Fig. 2. $\bar{\beta}$-Angular functions.

can be swapped in Eqs. (5) and (8) (and thus in Eqs. (14) and (15), leading to $K^*_{IIf} = K_{IIf}/K_{Ic}$), by considering a different definition for the dimensionless T-stress, namely $\tau_{II} = T\sqrt{l_{ch}}/K_{II}$. On the other hand, according to this choice, problems would rise as pure mode I is approached ($K_{II} \to 0, \psi \to 0^\circ$), since τ_{II} diverges.

In order to overcome these drawbacks, a novel approach is here considered, referring to τ_I for $0^\circ \le \psi \le 45^\circ$ (mode I – dominated zone) and to τ_{II} and for $45^\circ \le \psi \le 90^\circ$ (mode II – dominated zone). Observe that the condition $\tau_I = \tau_{II}$ for $\theta = 45^\circ$ guarantees the functions to be continuous.

3. FFM results

FFM results are presented in Figs. 3 and 4, for the fracture loci and the critical kinking angle, respectively. By assuming $K_I,\ K_{II} > 0$, as T increases, the failure load decreases, while the critical kinking angle $|\theta_c|$ increases, tending asymptotically towards 90°. This behavior can be detected directly from Eq. (15): for a sufficiently high $\tau_I,\ K^*_{If} \to 1/\tau_I \sin^2\theta$. The critical load thus results independent of ψ and of δ, and the critical kinking angle coincides with the maximum of the function $\sin^2\theta$, i.e. $|\theta_c| = 90^\circ$, Fig. 4.

As concerns pure mode I loading conditions ($K_{II} = 0$), if $T > 0$ is sufficiently large, the crack does not propagate collinearly any more ($\theta_c \neq 0^\circ$) and K^*_{If} deviates from the unit value. This phenomenon has been already described in the Literature [6,18,22] and is investigated more in details through FFM in Fig. 5. The present results, showing continuous functions, are in agreement with those derived in [18], but slightly differ from those proposed in [22] where the existence of a $|\theta_c|$-jump from 0° to 72° was detected for a threshold tensile T. On the other hand, in the case of a compressive T-stress ($T < 0$), the straight crack path always reveals to be stable [6,22].

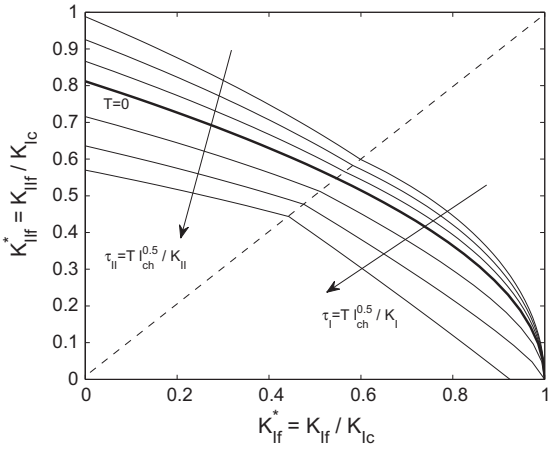

Fig. 3. T-stress effects on FFM fracture loci. From the top to the bottom, curves refer to $\tau_i (i = I, II) = -0.1, -0.2, -0.3, 0$ (thick line), 0.2, 0.4, 0.6. The dotted line represents the condition $K_I = K_{II}$, according to which $\tau_I = \tau_{II}$.

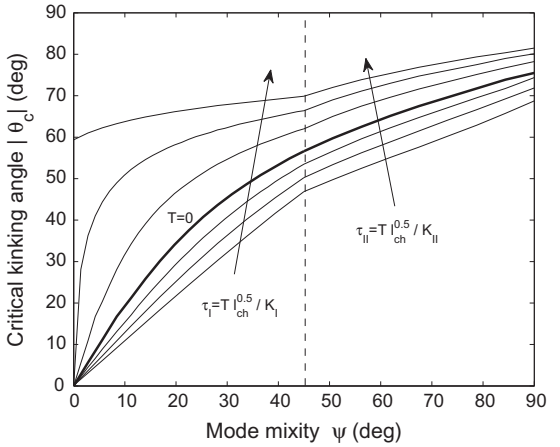

Fig. 4. T-stress effects on FFM critical kinking angle. From the bottom to the top, curves refer to $\tau_i\,(i = I, II) = -0.1, -0.2, -0.3, 0$ (thick line), 0.2, 0.4, 0.6. The dotted line represents the condition $K_I = K_{II}$, according to which $\tau_I = \tau_{II}$.

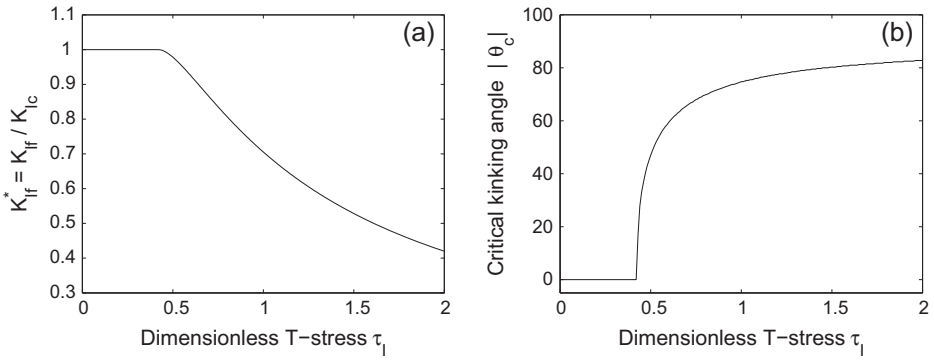

Fig. 5. FFM predictions, mode I : T-stress effects on the critical SIF (a) and on the critical kinking angle (b).

As regards (prevailing) mode *II* loading conditions ($K_I = 0$), an increasing tensile T-stress provides increasing kinking angles $|\theta_c|$ from 75.5° ($T = 0$, [32]) to 90° ($T \to \infty$). The trend is the same for compressive T-stress, but no solutions of Eq. (14) are obtained for $\tau_{II} < -0.3$. Looking for a possible explanation, the crack can not grow due to decreasing circumferential stresses, which affect both conditions (5) and (8). In such a case, a crack growth along the plane of maximum shear stress can be supposed. Indeed, mode *II*-crack growth in a brittle material is preferred if a sufficiently high confining pressure is present [33]; the crack can kink or propagate straight ahead, depending on the loading conditions [34]. Further studies are in progress.

Eventually, notice that a similar investigation to that shown was carried out in [18] by implementing the point stress criterion [15,16]. Nevertheless, results were presented considering a unique dimensionless T-stress, $\tau = T\sqrt{l_{ch}}/\sqrt{K_I^2 + K_{II}^2}$. Although intriguing, according to our opinion, this choice may reveal misleading, since τ depends clearly on the mode mixity ψ.

4. Experimental validation

In the previous section it has been shown (Figs. 3 and 4) that T-stress effects reveal to be more significant for sufficiently high T-magnitudes and (prevailing) mode *II* conditions, coherently with what found in [18]. Furthermore, also the material plays a key-role, since the T-contribution increases as less brittle materials are considered (i.e., higher l_{ch}). Before proceeding, let us underline that in common applications, since all the parameters T, K_I and K_{II} generally vary as ψ varies during a specific test, the real impact of T-stress on predictions should be discussed from case to case, after evaluating these three parameters.

In order to validate the FFM approach, theoretical predictions are now compared with experimental results. A large amount of data is available in the Literature: indeed, for criteria based on a critical distance, such as FFM, the crack advance must be sufficiently small with respect to the notch depth and to the characteristic specimen dimension. If these hypothesis are disregarded, neither the real stress field nor the SIFs of the kinked crack can be described accurately by Eqs. (4), (6) and (7).

In the present work, the results obtained by testing diagonally loaded square plate (DLSP) specimens made of PMMA [19] are firstly taken into account. The mode-mixity was varied by changing the central crack inclination with respect to the applied load direction. The following material properties are considered: $K_{Ic} = 1.33$ MPa $\sqrt{\text{m}}$ and $\sigma_u = 120$ MPa (thus $l_{ch} \simeq 0.12$ mm). While the former value was given in [19], the latter was neither measured nor provided explicitly. It is here derived from a best-fit procedure on FFM predictions over a typical range for PMMA (70–130 MPa, [35,27]).

Functions K_I, K_{II} and T can be evaluated numerically through one of the techniques proposed in the Literature [36,11,22]. Indeed, their values are here extracted from the tables and the graphics presented in [19], for the sake of simplicity: units for K_I (K_{II}) and T are MPa $\sqrt{\text{m}}$ and MPa, respectively. The resulting values for τ_I and τ_{II} are reported in Table 1: notice that T is always negative, except for $\psi = 90°$ (prevailing mode *II*), and that its contribution is minimum for $\psi = 58.3°$.

FFM results are displayed in Fig. 6, as concerns the fracture loci (a) and the critical kinking angle (b). As can be seen, T-stress effects slightly improve predictions for high mixity-ratios, the maximum percentage improvements, nearly 2%, being generally observed for $\psi = 90°$. In Fig. 6, results related to the point stress (PS) or maximum tangential stress (MTS) criterion are also reported: the approach is based on the simple condition $\sigma_{\theta\theta}(r = r_c) = \sigma_u$, with $r_c = l_{ch}/(2\pi)$. The PS criterion including T-stress is named as 'Generalized Maximum Tangential Stress' (GMTS) criterion in [18,19]. Notice from Fig. 6 that FFM generally provides higher values as concerns the failure load and lower values as regards the critical kinking angle with respect to the PS approach. Indeed, theoretical predictions do not differ significantly from each other and they show a similar trend by including T-stress.

As a second example, in order to face cases where the T-contribution reveals more evident, we consider the experimental tests carried out on PMMA large plane slabs [4]. They were loaded by a remote uniaxial traction σ, with a central through-thickness crack forming an angle α with the force direction. The same test was also performed in [3], but on samples with different geometrical dimensions.

Table 1
PMMA cracked samples [19]: values for τ_I and τ_{II}.

ψ (deg)	0	18	36.8	58.3	90
τ_I	−0.102	−0.0978	−0.0860	−0.0368	–
τ_{II}	–	−0.301	−0.115	−0.0277	0.0912

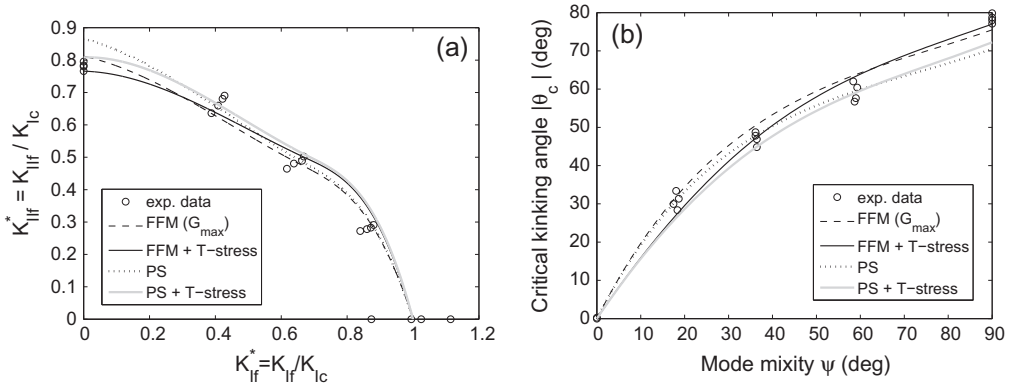

Fig. 6. FFM and PS (MTS) predictions on PMMA cracked samples [19]: *T*-stress effects.

Several inclination angles, corresponding to $\alpha = 0°$, 5°, 15°, 30°, 45°, 60°, 75° and 90°, were considered in [4]. Notice that, for what concerns the first three cases, the material failure was found to occur prior to the crack branching and the critical kinking angles were not measured [5]. Modeling the present geometry as if it were infinite, K_I, K_{II} and T can be expressed analytically as:

$$K_I = \sigma\sqrt{\pi a}\sin^2\alpha,$$

$$K_{II} = \sigma\sqrt{\pi a}\sin\alpha\cos\alpha,$$

$$T = \sigma\cos 2\alpha,$$

being a the crack half-length. Pure mode *I* is recovered for $\alpha = 90°$, while T is the only stress term different from zero for $\alpha = 0°$, since both mode *I* and mode *II* SIFs vanish. Furthermore, T is positive for $0° \leqslant \alpha \leqslant 45°$ ($0° < \alpha \leqslant 45°$ representing mode *II* dominated zone) and negative for $45° \leqslant \alpha \leqslant 90°$ (mode *I* dominated zone).

FFM predictions are reported in Fig. 7 as concerns the fracture loci (a) and the critical kinking angle (b), by implementing $K_{Ic} = 2.94$ MPa $\sqrt{\text{m}}$ and $\sigma_u = 80$MPa ($l_{ch} \simeq 1.3$ mm). While the former value was obtained experimentally in [4], the latter is again fitted, its value resulting a little higher than the critical stress measured for $\alpha = 0°$-inclined samples. From Fig. 7 it can be seen that theoretical predictions are significantly improved by considering *T*-stress effects, especially as concerns the fracture loci for low α-values.

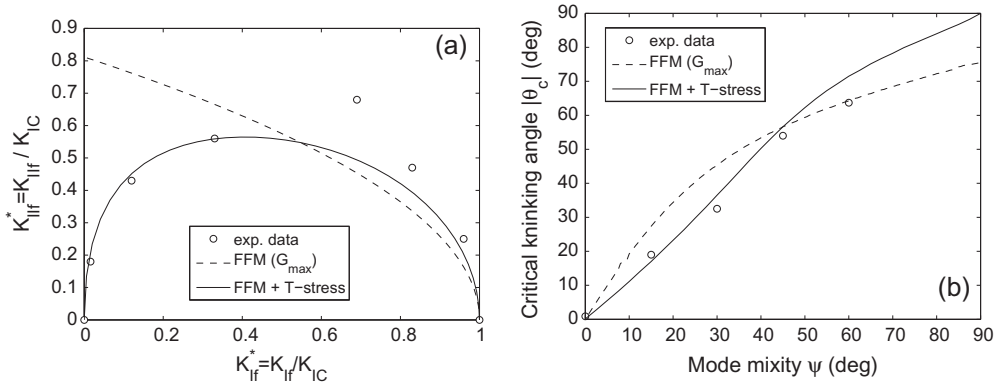

Fig. 7. FFM predictions on PMMA cracked slabs [4]: *T*-stress effects.

Eventually, it is important to mention the large amount of experimental tests recently carried out (see for instance [37] and related references) on rock materials. These are less brittle than PMMA: the related critical distance results obviously larger, and, as outlined before, also *T*-stress effects become more significant. We have considered the data presented in [37], related to triangular Neiriz marble samples ($K_{Ic} = 1.23$ MPa $\sqrt{\text{m}}$ and $\sigma_u = 5.64$ MPa, providing $l_{ch} \simeq 47$ mm) subjected to three-point bending loading. Indeed, FFM predictions are rather poor even by including *T*-stress effects and the comparison is not presented in this work. The huge deviation found is imputable to the fact that the crack advance is not sufficiently small with respect to the notch depth (revealing to be even larger): failure load predictions result thus underestimated. Analogous considerations hold also for other tests on materials possessing similar mechanical properties (e.g., limestone rocks). In order to get more accurate estimations, higher order terms in the expansions (4), (6) and (7) or non-linear models must be taken into account: further studies are in progress.

5. Conclusions

T-stress affects failure predictions of brittle elements under mixed mode loading conditions, both as concerns the failure load and the critical kinking angle. In the present work, this problem was investigated through FFM, by means of a semi-analytical approach. An original way of displaying results was proposed, referring to two different definitions of the dimensionless *T*-stress: the most suitable choice depends on which mode, between mode *I* and mode *II*, prevails. The satisfactory comparison with PMMA experimental data concluded the paper.

References

[1] Erdogan F, Sih GC. On the crack extension in plates under plane loading and transverse shear. J Basic Engng 1963;85:519–25.
[2] Hussain M, Pu S, Underwood J. Strain energy release rate for a crack under combined mode I and mode II. In: Fracture analysis, ASTM-STP 560, Am Soc Testing Materials; 1974.
[3] Williams JG, Ewing PD. Fracture under complex stress the angled crack problem. Int J Fract Mech 1972;8:441–6.
[4] Carpinteri A. Crack dominante e microcracks nei material fragili (IN ITALIAN). Giorn Genio Civ 1-2-3 1978:67–82.
[5] Carpinteri A, DiTommaso A, Viola E. Collinear stress effect on the crack branching phenomenon. Mat Constr 1979;12:439–46.
[6] Cotterell B, Rice JR. Slightly curved or kinked cracks. Int J Fract 1980;16:155–69.
[7] Leevers PS, Radon JC. Inherent stress biaxiality in various fracture specimen geometries. Int J Fract 1982;19:311–5.
[8] Yukio U, Kazuo I, Tetsuya Y, Mitsuru A. Characteristics of brittle fracture under general combined modes including those under bi-axial tensile loads. Engng Fract Mech 1983;18:1131–58.
[9] He MY, Bartlett A, Evans AG, Hutchinson JW. Kinking of a crack out of an interface: role of in-plane stress. J Am Ceram Soc 1991;74:767–71.
[10] Becker TL, Cannon RM, Ritchie RO. Finite crack kinking and *T*-stresses in functionally graded materials. Int J Solids Struct 2001;38:5545–63.
[11] Glaucio J-HK, Paulino H. *T*-stress, mixed-mode stress intensity factors, and crack initiation angles in functionally graded materials: a unified approach using the interaction integral method. Comput Methods Appl Mech Engng 2003;192:1463–94.
[12] Christopher CJ, James MN, Patterson EA, Tee KF. Towards a new model of crack tip stress fields. Int J Fract 2007;148:361–71.
[13] Lazzarin P, Berto F, Radaj D. Fatigue-relevant stress field parameters of welded lap joints: pointed slit tip compared with keyhole notch. Fatigue Fract Engng Mater Struct 2009;32:713–35.
[14] Berto F, Lazzarin P. On higher order terms in the crack tip stress field. Int J Fract 2010;161:221–6.
[15] Ritchie RO, Knott JF, Rice JR. On the relationship between critical stress and fracture toughness in mild steel. J Mech Phys Solids 1973;21:395–410.
[16] Kosai M, Kobayashi AS, Ramulu M. Tear straps in airplane fuselage. In: Durability of metal aircraft structures. Atlanta Technology Publications; 1993.
[17] Seweryn A. A non-local stress and strain energy release rate mixed mode fracture initiation and propagation criteria. Engng Fract Mech 1998;59:737–60.
[18] Smith DJ, Ayatollahi MR, Pavier MJ. The role of T-stress in brittle fracture for linear elastic materials under mixed-mode loading. Fatigue Fract Engng Mater Struct 2001;24:137–50.
[19] Ayatollahi MR, Aliha MRM. Analysis of a new specimen for mixed mode fracture tests on brittle materials. Engng Fract Mech 2009;76:1563–73.
[20] Pugno N, Ruoff R. Quantized fracture mechanics. Philos Mag 2004;84:2819–45.
[21] Leguillon D. Strength or toughness? a criterion for crack onset at a notch. Eur J Mech A/Solids 2002;21:61–72.
[22] Leguillon D, Murer S. Crack deflection in a biaxial stress state. Int J Fract 2008;150:75–90.
[23] Leguillon D. Asymptotic and numerical analysis of a crack branching in non-isotropic materials. Eur J Mech A/Solids 1993;12:33–51.
[24] Cornetti P, Pugno N, Carpinteri A, Taylor D. Finite fracture mechanics: a coupled stress and energy failure criterion. Engng Fract Mech 2006;73:2021–33.
[25] Carpinteri A, Cornetti P, Pugno N, Sapora A, Taylor D. Generalized fracture toughness for specimens with re-entrant corners: experiments vs. theoretical predictions. Struct Engng Mech 2009;32:609–20.
[26] Carpinteri A, Cornetti P, Sapora A. Brittle failures at rounded V-notches: a finite fracture mechanics approach. Int J Fract 2011;172:1–8.
[27] Sapora A, Cornetti P, Carpinteri A. A finite fracture mechanics approach to V-notched elements subjected to mixed-mode loading. Engng Fract Mech 2013;97:216–26.
[28] Tada H, Paris PC, Irwin GR. The stress analysis of cracks handbook. Paris Productions Incorporated; 1985.
[29] Melin S. Accurate data for stress intensity factors at infinitesimal kinks. J Appl Mech 1994;61:467–70.
[30] Cornetti P, Sapora A, Carpinteri A. Mode mixity and size effect in V-notched structures. Int J Solids Struct 2013;50:1562–82.
[31] Fett T, Pham VB, Bahr HA. Weight functions for kinked semi-infinite cracks. Engng Fract Mech 2004;71:1987–95.
[32] Sapora A, Cornetti P, Carpinteri A. V-notched elements under mode II loading conditions. Struct Engng Mech 2014;49:499–508.
[33] Melin S. Fracture from a straight crack subjected to mixed-mode loading. Int J Fract 1987;32:257–63.
[34] Isaksson P, Ståhle P. Mode II crack paths under compression in brittle solids a theory and experimental comparison. Int J Solids Struct 2002;39:2281–97.
[35] Seweryn A, Lukaszewicz A. Verification of brittle fracture criteria for elements with V-shaped notches. Engng Fract Mech 1998;69. 14877-1510.
[36] Ayatollahi MR, Pavier MJ, Smith DJ. Determination of *T*-stress from finite element analysis for mode *I* and mixed mode *I*/*II* loading. Int J Fract 1998;91:283–98.
[37] Aliha MRM, Hosseinpour GR, Ayatollahi MR. Application of cracked triangular specimen subjected to three-point bending for investigating behavior of rock materials. Rock Mech Rock Engng 2013;46:1023–34.